

# Ductility and limit states

Autor(en): **Marinek, M.**

Objektyp: **Article**

Zeitschrift: **IABSE congress report = Rapport du congrès AIPC = IVBH  
Kongressbericht**

Band (Jahr): **9 (1972)**

PDF erstellt am: **21.07.2024**

Persistenter Link: <https://doi.org/10.5169/seals-9538>

## **Nutzungsbedingungen**

Die ETH-Bibliothek ist Anbieterin der digitalisierten Zeitschriften. Sie besitzt keine Urheberrechte an den Inhalten der Zeitschriften. Die Rechte liegen in der Regel bei den Herausgebern.

Die auf der Plattform e-periodica veröffentlichten Dokumente stehen für nicht-kommerzielle Zwecke in Lehre und Forschung sowie für die private Nutzung frei zur Verfügung. Einzelne Dateien oder Ausdrucke aus diesem Angebot können zusammen mit diesen Nutzungsbedingungen und den korrekten Herkunftsbezeichnungen weitergegeben werden.

Das Veröffentlichen von Bildern in Print- und Online-Publikationen ist nur mit vorheriger Genehmigung der Rechteinhaber erlaubt. Die systematische Speicherung von Teilen des elektronischen Angebots auf anderen Servern bedarf ebenfalls des schriftlichen Einverständnisses der Rechteinhaber.

## **Haftungsausschluss**

Alle Angaben erfolgen ohne Gewähr für Vollständigkeit oder Richtigkeit. Es wird keine Haftung übernommen für Schäden durch die Verwendung von Informationen aus diesem Online-Angebot oder durch das Fehlen von Informationen. Dies gilt auch für Inhalte Dritter, die über dieses Angebot zugänglich sind.

## Ductility and Limit States

Ductilité et états limites

Duktilität und Grenzzustände

M. MARINČEK

Professor at the University of Ljubljana  
Jougoslavia

**INTRODUCTION** The limit states of the load carrying members and structures clearly can be treated with the help of the typical load-displacement diagram, obtained experimentally, or with the elasto-plastic theory, which enables the prediction of the real deformational behaviour. With this theory any shape of the stress-strain diagram of the material and the influence of the residual stresses can be taken into account. So the instability loads and/or the suitable defined inelastic deflection limit load can be established. Various secondary and local effects like lateral instability, local instability, ductile, brittle, and fatigue fracture have to be referred to the primary global elasto-plastic behaviour. The reliability of different approximate design methods may be estimated by correlating them to the elasto-plastic behaviour. The dimensionless treatment ( which represents also the model law for experimental work ) and the appropriate classification make possible the wider use of the results of the elasto-plastic theory.

In this article the inplanar treatment for the single loading of simple linear structures with time independent inelastic material behaviour is presented.

**DUCTILITY FUNCTIONS OF THE CROSS-SECTION** The nonlinear relationship between the internal force and corresponding specific deformation of the axe of the bar can be expressed in the general case by

$$\begin{aligned} \varphi_x &= \frac{M_x}{EI_x} K_{\varphi x} & \varphi_y &= \frac{M_y}{EI_y} K_{\varphi y} & \varepsilon &= \frac{N}{EA} K_{\varepsilon} \\ \gamma_x &= \frac{\partial x Q_x}{EA} K_{\gamma x} & \gamma_y &= \frac{\partial y Q_y}{EA} K_{\gamma y} & \theta &= \frac{T}{EJ} K_{\theta} \end{aligned} \quad (1)$$

where the ductility function of the cross-section  $K$  can depend on all internal forces,  $K_i = f ( M_x, M_y, Q_x, Q_y, N, T )$ . Dimensionless, for the case of uniaxial bending<sup>1</sup> with the normal force, there is

$$K_{\varphi} = f ( \bar{M}, \bar{N} ) \quad (2)$$

with  $\bar{M} = M : M^0$  and  $\bar{N} = N : N^0$ , where  $M^0$  and  $N^0$  are typical internal forces ( referred to the proportional limit, yield strength limit, or compression strength of material ). Using the Bernoulli hypothesis for the chosen strains over the cross-section,  $M$  and  $N$  are obtained with the corresponding integration for a given stress-strain diagram of material.

For the stress-strain diagram after Ramberg-Osgood  $\bar{\varepsilon} = \bar{\sigma}(1 + \bar{\sigma}^n)$ , with  $\bar{\varepsilon} = \varepsilon : \varepsilon^0$ ,  $\bar{\sigma} = \sigma : \sigma^0$ , where  $\varepsilon^0 = \sigma^0 : E$  and the yield strength  $\sigma^0$ , defined in Fig.1, the curves in Fig.2 with different parameters  $n$  represent four typical dimensionless stress-strain behaviour. For  $n = 10$  and the rectangular

cross-section the ductility functions  $K_\varphi$  are given in Fig.3, full lines for strain reversal with constant  $\bar{N}$ , and the dashed ones for nonlinear elastic material.

There is a simple relationship between the ductility functions of the individual parts of the cross-section and those of the whole composite one;

$$K_\varphi = \frac{\sum_n EI}{\sum_n \frac{EI}{K_\varphi}} \quad (3)$$

In this way calculated ductility functions for bending and compression of a concrete filled tube are presented in Fig.4, for an ideal elastic-ideal plastic stress-strain diagram of steel and according to CEB for concrete. The typical internal forces are here

$$M^0 = \frac{\pi}{32} [\sigma_s^0 (D^3 - d^3) + \sigma_c^0 d^3] \quad N^0 = \frac{\pi}{4} [\sigma_s^0 (D^2 - d^2) + \sigma_c^0 d^2]$$

DUCTILITY FUNCTIONS OF THE LOAD CARRYING MEMBERS The typical elasto-plastic load-displacement diagram can be performed for example with

$$\delta = \int_0^s \frac{MM_v}{EI} K_\varphi ds \quad (4)$$

One can replace the influence of  $K_\varphi$  with

$$\frac{EI}{K_\varphi} = EI_{eff} = E_{eff} I = (EI)_{eff},$$

but the ductility factor  $K_\varphi$  has a clearer meaning, especially for composite cross-section.

Similar to the definition of  $K_\varphi$ , the ductility of the load carrying member, or structure  $K_\delta$ , is the ratio between the elasto-plastic displacement and the corresponding elastic one,

$$K_\delta = \delta : \delta^e. \quad (5)$$

Consequently, the relationship between the dimensionless load  $\bar{P} = P : P^0$  and dimensionless displacement  $\bar{\delta} = \delta : \delta^e$ , where  $P^0$  represents for example the limit state according to the theory of elasticity, and  $\delta^e$  the corresponding elastic displacement, is

$$\bar{\delta} = \bar{P} \cdot K_\delta. \quad (6)$$

SOME EXAMPLES For the simple beam with constant properties along the axis there is the deflection under concentrated load, acting in any point,

$$K_\delta = \frac{3}{P^0} \int_0^{\bar{P}} \bar{M}^2 K_\varphi d\bar{M}, \quad (7)$$

for the uniformly distributed load on a beam

$$K_{\delta} = \frac{6}{5\bar{P}^2} \int_0^{\bar{P}} \left( \frac{1}{\sqrt{1 - \frac{\bar{M}}{\bar{P}}}} - 1 \right) \bar{M} K_{\varphi} d\bar{M}, \quad (8)$$

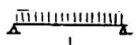
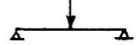
and on a cantilever

$$K_{\delta} = \frac{2}{\bar{P}^2} \int_0^{\bar{P}} \bar{M} K_{\varphi} d\bar{M}, \quad (9)$$

with  $\bar{P} = \bar{M}_{\max}$ . Fig.5 shows the results for the rectangular cross-section and three different stress-strain diagrams with strain hardening.

For the examples in Fig.6 the dimensionless deflection limit load  $\bar{P}_{1,1}$ , defined with 10% irreversible deflection and the plastic hinge load, both related to the elastic limit loads, are presented in the table I. Thus there is the possibility for higher allowable stresses in elastic design, dependent on the cross-section and loading ( in this case for the material with  $n = \infty$ , without residual stresses ).

Table I

	●	■	D/t=20	D/t=∞	IPB <sub>V</sub> 100	IPB <sub>V</sub> 340	IPB <sub>L</sub> 300	
	1,43	1,31	1,23	1,17	1,21	1,14	1,08	$\bar{P}_{1,1}$
	1,54	1,39	1,29	1,22	1,23	1,16	1,10	$\bar{P}_{1,1}$
	1,70	1,50	1,34	1,27	1,24	1,16	1,10	$\bar{P}^{\bullet}$

The symmetric continuous beam, loaded as in Fig.7, has the ductility function

$$K_{\delta} = \frac{6(3+2\lambda)}{(3+10\lambda)(\bar{M}_1 + \bar{M}_2)} \left( \int_{\bar{M}_2}^{\bar{M}_1} \bar{M} K_{\varphi} d\bar{M} + 4\lambda \frac{\bar{M}_1 + \bar{M}_2}{\bar{M}_1^2} \int_0^{\bar{M}_1} \bar{M}^2 K_{\varphi} d\bar{M} \right), \quad (10)$$

with

$$\int_0^{\bar{M}_2} \frac{\bar{M} K_{\varphi} d\bar{M}}{\sqrt{1 - \frac{\bar{M}}{\bar{M}_2}}} = \int_0^{\bar{M}_1} \frac{\bar{M} K_{\varphi} d\bar{M}}{\sqrt{1 + \frac{\bar{M}}{\bar{M}_2}}} + \frac{4\lambda}{\bar{M}_1^2} \sqrt{(\bar{M}_1 + \bar{M}_2) \bar{M}_2} \int_0^{\bar{M}_1} \bar{M}^2 K_{\varphi} d\bar{M}$$

as the deformational condition. There is strong dependence on  $\lambda$ , the ratio of spans.

Fig.8 shows for  $\lambda = 1$  the influence of different stress-strain parameters  $n$ , compared with the plastic hinge theory, and Fig.9 the influence of the cross-section properties for  $\lambda = 0$ .

In Fig.10 the load carrying capacities are given for a beam-column, made of the material with  $n = 10$ , as the function of the slenderness  $\lambda$ . The dashed lines represent the influence of strain reversal at  $\bar{N} = \text{const}$  and growing  $\bar{Q}$ .

In Fig.11 the elasto-plastic load deflection diagram  $\bar{Q} - \bar{\delta}$  for  $\bar{N} = 0,1$  for different parameter  $n$  of material can be compared with those of the second order elastic theory and the second order plastic hinge theory. Similarly in Fig.13 for  $\bar{N} = 0,25$  and in Fig.14 for  $\bar{N} = 0,525$  are  $\bar{Q} - \bar{\delta}$  curves for weak axial bending of DIE20, material with  $n = \infty$ , dashed curves for the presence of residual stresses and nonhomogeneity, dimensionless given in Fig.12. For higher  $\lambda$  and higher  $\bar{N}$  the difference between elastic limit load, plastic hinge limit load, and elasto-plastic instability limit load, with and without residual stresses, are substantial.

For the case when  $Q = \text{const}$ , in Fig.15 and 16, the relationship  $\bar{N} - \bar{\delta}$  is presented for the material with  $n = \infty$  and the rectangular cross-section.

In Fig.15 for  $\bar{Q} = 0,5$  there exists the elastic limit curve and the plastic hinge curve, whereas in Fig.16 the value  $\bar{Q} = 1$  alone represents already the elastic limit state, but for all that there is a large additional normal force carrying capacity, particularly for lower slendernesses.

The dimensionless buckling curves for column with the composite cross-section can be represented in the same diagram as for columns with the single material. So in Fig.17 the lower curve is the tangent modulus curve for the plain concrete, CEB stress-strain diagram, and the upper curve is the Euler curve for the ideal elastic - ideal plastic diagram of steel. Three curves in between belong to columns with concrete filled tubes and encased I-profile ( numbers describe the steel cross-section, steel yield strength, and concrete compression strength ). The slenderness of concrete filled steel tube is

$$\bar{\lambda} = \frac{4L}{\pi D} \sqrt{\frac{1 + c \frac{G_c^p}{G_s^p}}{1 + c \frac{E_c}{E_s}}} \quad \text{with} \quad c = \frac{1}{\frac{D^4}{d^4} - 1} \quad (11)$$

Of course, the real columns have geometrical and structural imperfections. Therefore, the corresponding instability limit loads with the help of the beam-column elasto-plastic theory have to be determined. Fig.18 gives the  $\bar{Q} - \bar{\delta}$  curves with the instability limit states for different slender beam-columns with concrete filled tube cross-section, having ductility functions in Fig.4.

FINAL REMARKS The consequent dimensionless treatment would have larger effects in using the results of the elasto-plastic theory for better understanding of the ductile behaviour of structures and with this more rational use of material.

The deterministic treatment of structures with the elasto-plastic theory supports and supplies the probabilistic treatment because a significant variation is possible only with representative parameters for separated influences. On the contrary, the pure empirical statistical analysis of the complex phenomena appearing in the ductile behaviour of structures is rather questionable, if not impossible.

The extension of the elasto-plastic theory on the problems, taking into account more complicated loading and structural geometry, the Bauschinger effect, the influence of the temperature ( also fire ), and strain velocity, calls even more attention to the international collaboration in finding the appropriate classification of the shapes for stress-strain diagrams of the material, cross-sections, structural and geometrical imperfections.

AKNOWLEDGEMENT Some results are presented here from larger research project, carried out with the financial support by "Boris Kidrič" Foundation of Ljubljana. The collaboration with my past and present assistant P.Fajfar, V.Marolt, J.Reflak and M.Vitek, and also numerous students, is very much appreciated.

SUMMARY Presented results of the elasto-plastic theory, compared with the corresponding elastic theory and plastic hinge theory, show on the one side, that the possibility exists for better exploitation of material also for statical determined structures when inelastic deflection limit state has to be decisive, and on the other side, that one should be careful with the unlimited use of the plastic hinge theory for stability limit states.

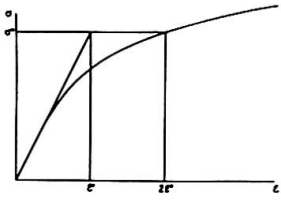


Fig. 1

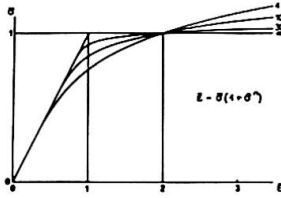


Fig. 2

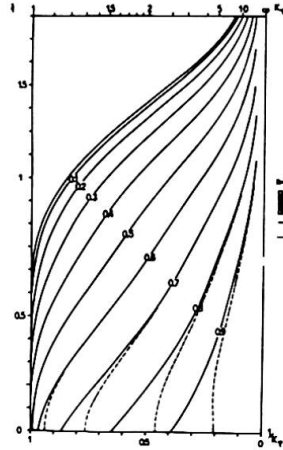


Fig. 3

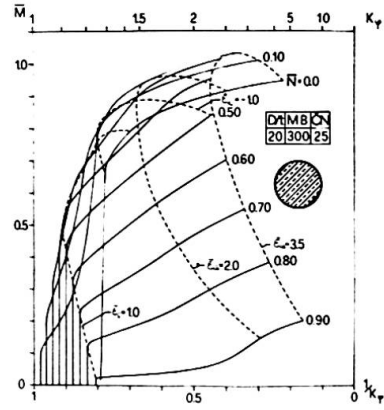


Fig. 4

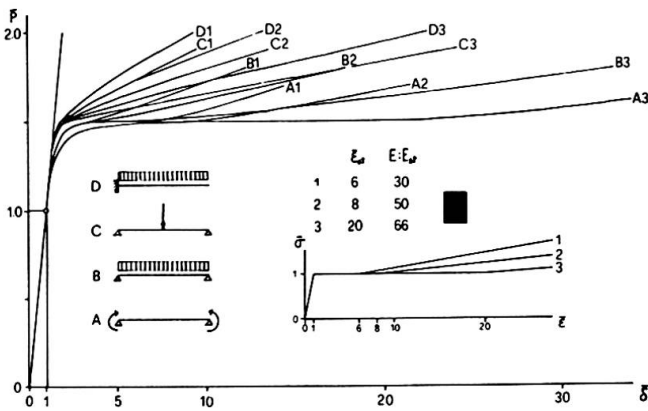


Fig. 5

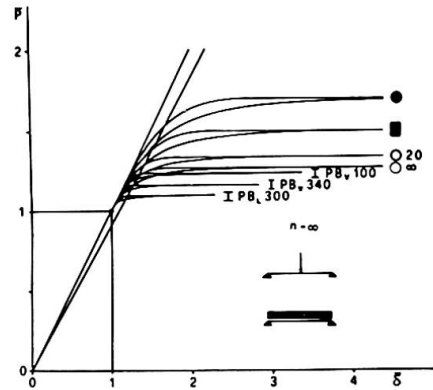


Fig. 6

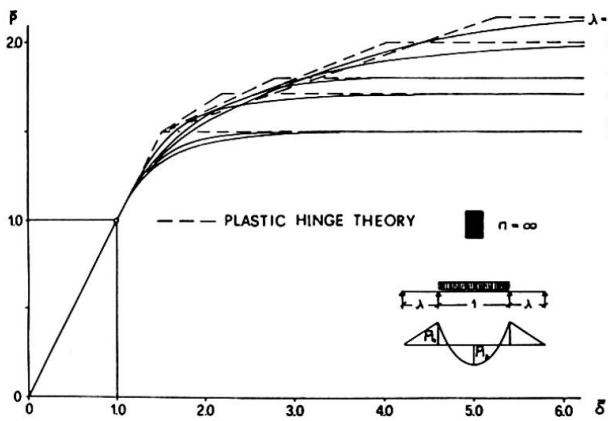


Fig. 7

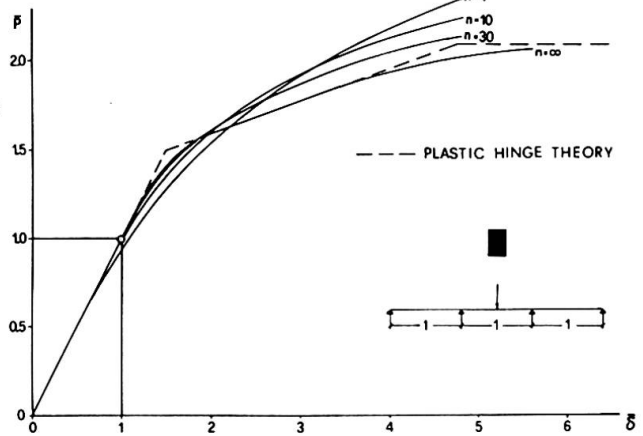


Fig. 8

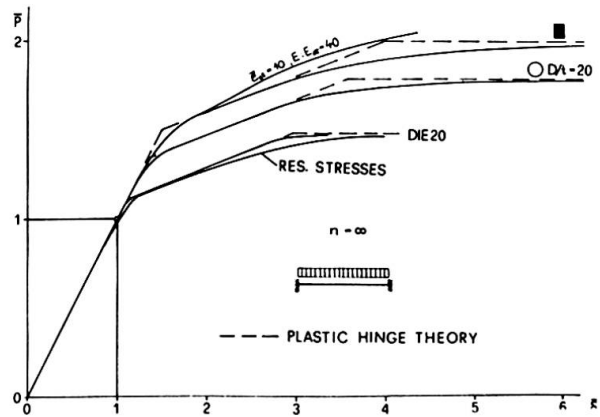


Fig. 9

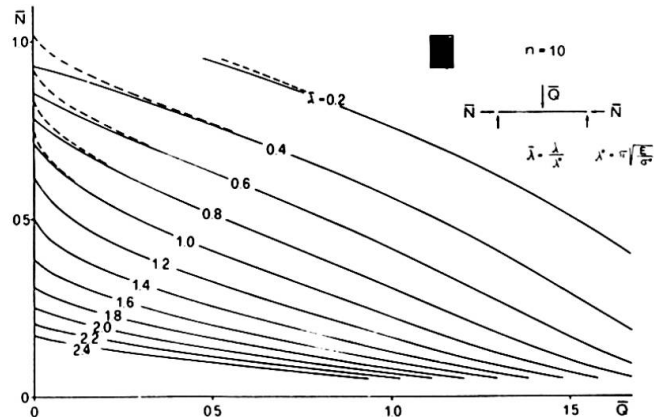


Fig. 10

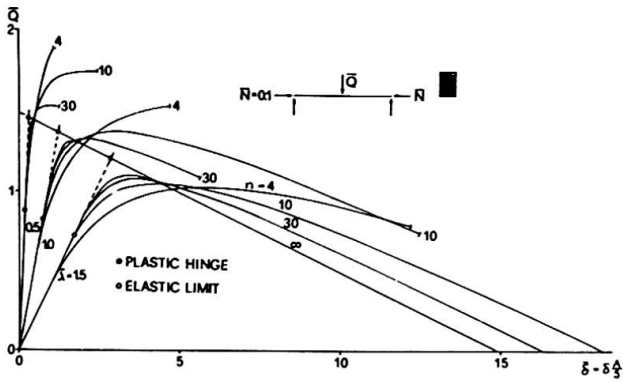


Fig. 11

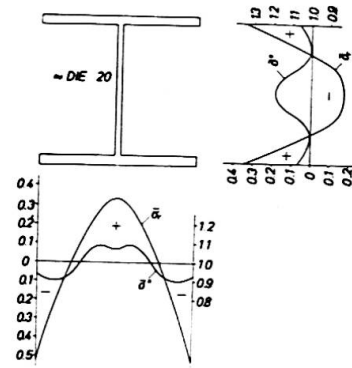


Fig. 12

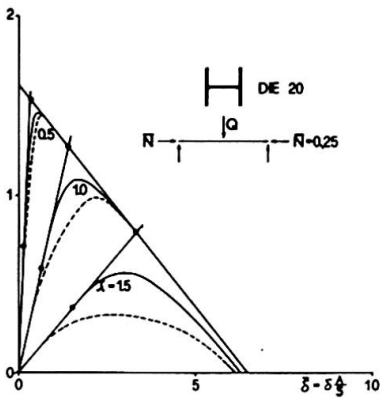


Fig. 13

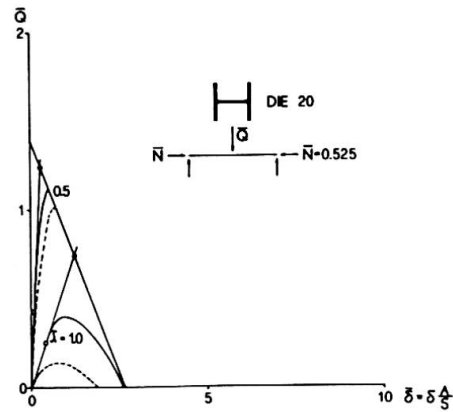


Fig. 14

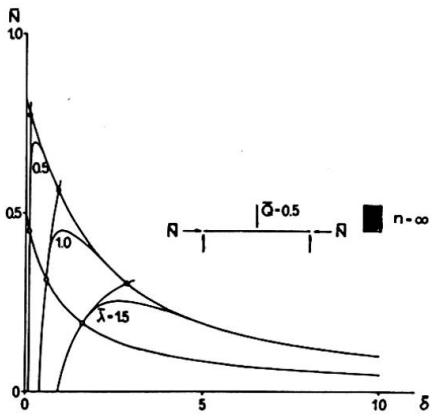


Fig. 15

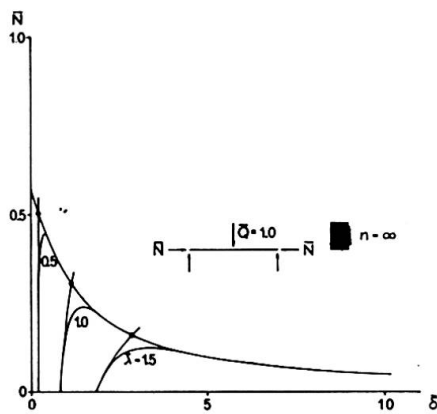


Fig. 16

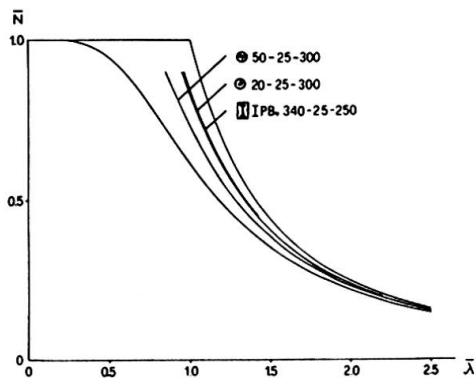


Fig. 17

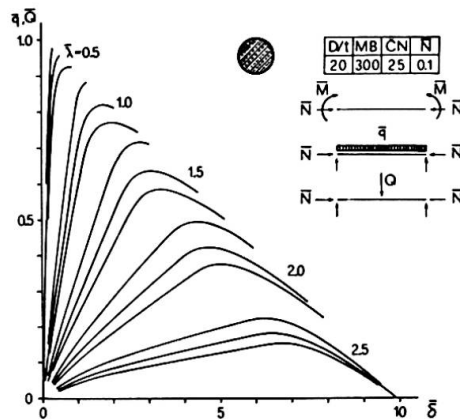


Fig. 18